

Single-Particle Excitations in Magnetic Insulators

W. F. Brinkman and T. M. Rice

Bell Telephone Laboratories, Murray Hill, New Jersey 07974

(Received 5 March 1970)

In this paper, the density of states and the mobility of an extra electron or hole are calculated in the atomic limit of the Hubbard model. Both the half-filled single-band and multiple-band situations are discussed. The problem is formulated in terms of the number of paths which return to the origin leaving the spin configuration unchanged. The density of states then depends on spin configuration and we have considered the random (R) (high-temperature) and antiferromagnetic (AF) arrangements. Examination of the first five nonzero moments for the simple cubic lattice indicates that the bands are narrowed by a factor of 0.745 (AF) and 0.805 (R). However, the exact bands have tails extending out to the full free-particle width for both spin arrangements. An approximate one-particle Green's function is obtained by summing all graphs with no closed loops. Such paths give a density of states that is independent of spin arrangement and is relatively flat with a sharp square-root edge at $2(z-1)^{1/2}t$. Here z is the coordination number and t is the nearest-neighbor hopping integral. Within this approximation, we have calculated the mobility of an extra hole and have found typical values to be $\sim 1 \text{ cm}^2/\text{V sec}$ so that the mobility is rather small, even though the density of states has a width of order $\sim 1 \text{ eV}$. Intra-atomic exchange is shown to give a further narrowing of the band [a factor of $(2)^{-1/2}$ in the two-band large-intra-atomic-exchange example]. The effect of finite t/U is considered, where U is the intra-atomic Coulomb interaction, and is shown to have a strong effect on the band tail but relatively weak effects on the bulk of the band. Finally, we make a few remarks comparing our results with the observed mobilities in NiO and the relevance of intra-atomic exchange to the behavior of the dioxide and sesquioxide series.

I. INTRODUCTION

In recent years there has been considerable interest in the electron states in localized magnetic insulators.¹⁻³ In this class of materials, the band theory of the conduction electrons breaks down because of the very strong Coulomb repulsion between the electrons. A model Hamiltonian which incorporates both the Coulomb repulsion and the kinetic energy for these narrow-band materials has been put forward by Hubbard.⁴ This model uses a Wannier representation for the electron states and retains only the Coulomb repulsion between electrons on the same lattice site. In this paper we shall examine this model in the atomic limit in which the transfer energy t is taken as much smaller than the Coulomb repulsion U , and discuss the density of states and mobility of an extra carrier.

The atomic limit of the Hubbard model with one electron per atom has been studied previously by Harris and Lange.⁵ These authors have shown that the one-particle spectral weight function has a series of bands separated in energy by U . They also showed that the values of the first three moments for the lowest two of these bands are unchanged from that of the tight-binding band. Nagaoka⁶ has formulated the Hubbard model in this limit in terms of the number of possible paths on a lattice and has shown that the ground state of the system with a small number of holes (or electrons)

is ferromagnetic. We shall make extensive use of his formulation in this work. We shall consider only the simple cubic lattice, though our results may be generalized to other lattices.

In Sec. II, the form of the density of states for a single hole (or electron) in a half-filled one-band Hubbard model in the atomic limit is examined. The first five nontrivial moments are calculated exactly using Nagaoka's path formulation.⁶ The values of the moments higher than the second depend on the spin configuration of the $N-1$ remaining electrons. Three configurations are examined: (i) ferromagnetic (F) in which case, as Nagaoka⁶ has shown, the problem reduces at once to that of a simple tight-binding band; (ii) antiferromagnetic (AF) by which we will mean the simple up-down spin configuration neglecting any zero-point spin deviation; and (iii) random (R) an average over all possible spin configurations with equal probability. From a knowledge of the moments, an approximate value of the band edge can be obtained by extrapolation, and it is found that the band is narrowed by approximately 20% (R) and 25% (AF) from the full (F) value. We argue, however, that there will be a band tail reaching all the way to the full ferromagnetic bandwidth which does not show up in the moment calculation. An approximate form for the density of states is obtained by using an expansion in Legendre polynomials. An analytic approximation for the Green's function of the hole is obtained

by summing all paths which are completely self-retracing and contain no closed loops. This approximation leads to a band which is narrowed by 25%, but without tails and which agrees well with the forms found from the Legendre polynomial fit to the moments especially in the AF case.

In Sec. III, the mobility of the hole is calculated. Since in the atomic limit all the spin configurations have zero energy, the hole is elastically scattered. Starting with the Kubo formula for the conductivity, we again keep only those paths which are completely self-retracing. The values obtained for the mobility are quite low ($\sim 1 \text{ cm}^2/\text{V sec}$ at $T \sim 1000^\circ \text{K}$), and it is argued that the carriers cannot be considered as propagating freely with weak scattering but rather undergo a diffusive Brownian motion through the lattice.

In Sec. IV, we consider the corrections to the atomic limit which are of order t/U . While these corrections appear to reduce the band tails considerably, their effect on the bulk of the band is small. We also generalize our results to a multiband situation and incorporate the effects of Hund's rule coupling. The same techniques as in Sec. II are used to analyze the limit in which both t/U and $t/J \rightarrow 0$, where J is the Hund's rule exchange energy. The qualitative features of the results are similar, with the bulk of band narrowed and with band tails. The bulk of the band is, however, farther narrowed by the Hund's rule coupling to give a combined reduction of $\approx 50\%$ (AF) and 70% (R) for a two-band model. The values of the mobility we calculate are not much affected by the inclusion of the Hund's rule coupling.

Finally, in the concluding section, we make some remarks on the relation of our results to experiment.

II. NATURE OF BANDS IN ATOMIC LIMIT OF THE HUBBARD MODEL

A. Formalism

In this section we will study the density of states for an extra electron or hole in a half-filled one-band Hubbard model in the atomic limit. We shall restrict ourselves to a simple cubic lattice, though the results which we shall obtain may be generalized in a straightforward manner to other simple lattice structures. The Hubbard Hamiltonian⁴ has the form

$$H = \sum_{ij\sigma} t_{ij} c_{i\sigma}^\dagger c_{j\sigma} + U \sum_i n_{i\uparrow} n_{i\downarrow}, \quad (2.1)$$

where $c_{i\sigma}^\dagger$ and $c_{i\sigma}$ denote, respectively, the creation and annihilation operators for an electron in a Wannier state localized at site i with spin σ , and $n_{i\sigma} (= c_{i\sigma}^\dagger c_{i\sigma})$ is the number operator for electrons with spin σ at the site i . The first term represents

the hopping of electrons from site j to i with an effective hopping integral t_{ij} . We shall consider only nearest-neighbor hopping so that $t_{ij} = t$ for nearest-neighbor sites, and $t_{ij} = 0$ for all other sites. The extension of the techniques which we use and the results which we obtain to include next-nearest neighbors is nontrivial, and we shall not consider the matter further. The second term represents the repulsive Coulomb interaction between two electrons on the same site. We shall restrict ourselves to the atomic limit in which $U \rightarrow \infty$. Consider a system with $N-1$ electrons distributed over N sites, i.e., a single hole in an otherwise half-filled band. (Because of the particle-hole symmetry of the model, we shall only discuss an extra hole.) For large values of U , the states of the system will be composed of a series of bands separated by an energy U corresponding to configurations with one hole, two holes, etc. In the atomic limit we need only consider the lowest band of states corresponding to configurations with only one hole, and we may ignore all terms in the Hamiltonian which link it to configurations with more than one hole. The manifold of states with one hole can be spanned by the set of states $\Psi_{i\alpha_i}$,

$$\Psi_{i\alpha_i} = (-1)^i c_{1\sigma_1}^\dagger c_{2\sigma_2}^\dagger \cdots c_{i-1\sigma_{i-1}}^\dagger c_{i+1\sigma_{i+1}}^\dagger \cdots c_N^\dagger \delta_N |0\rangle, \quad (2.2)$$

where α_i denotes the set $(\sigma_1, \sigma_2, \dots, \sigma_{i-1}, \sigma_{i+1}, \dots, \sigma_N)$ of possible spin configurations of the $N-1$ electrons and $|0\rangle$ is the vacuum state. The Hamiltonian H may be replaced by an effective Hamiltonian H' of the form

$$H' = Pt \sum_{ino} c_{i+n\sigma}^\dagger c_{i\sigma} P, \quad (2.3)$$

where n denotes the nearest neighbors of i , and P is a projection operator such that $P=1$, operating on a state with one hole, and $P=0$, otherwise.

The one-particle Green's function $G_{ij}^{\alpha_i \beta_j}(\omega)$ is defined as

$$G_{ij}^{\alpha_i \beta_j}(\omega) = \left\langle \Psi_{j\beta_j} \left| \frac{1}{\omega - H'} \right| \Psi_{i\alpha_i} \right\rangle. \quad (2.4)$$

Nagaoka⁶ has shown that poles of the one-particle Green's function $G_{ij}^{\alpha_i \beta_j}$ all lie on the real axes between $-zt$ and zt , where z is coordination number of the lattice. For the simple cubic lattice, $z=6$. The Green's function G depends on the α_i and we shall consider three sets of spin configurations: (R) random orientation of the spins, (AF) antiferromagnetic array of spins (we shall consider only the case of a simple antiferromagnet in which all six nearest-neighbor spins are aligned opposite to that on the central site), and (F) ferromagnetic alignment of all the spins. (We shall evaluate ex-

pectation values within a given spin arrangement and then average over all possible arrangements.) In the ferromagnetic case (F) the spin plays no role and the problem reduces at once to that of spinless electrons. The Green's function and density of states in this case have the well-known form for a single particle moving in a tight-binding band.

It is well known that Anderson kinetic exchange⁷ gives an antiferromagnetic coupling between nearest-neighbor spins of order t^2/U . In the atomic limit, the strength of this coupling goes to zero. This gives rise to problems associated with the degeneracy of the energy of the spin configuration which have been studied by a number of authors.⁸ Physically, our case (R), in which we average over all possible spin configurations α with equal probability, can be thought of as the finite-temperature atomic limit in which $U \gg t > kT \gg t^2/U$. The AF case can be arrived at if we take the limit $U \rightarrow \infty$ and $kT < t^2/U$, and neglect the zero-point spin deviation. Following Nagaoka⁶ we can consider the F case as the limit $U \rightarrow \infty$ at $T = 0^\circ\text{K}$ with the number of holes (or electrons) held fixed and finite.

B. Moment Expansion for Density of States

Nagaoka⁶ has pointed out that the Green's function $G(\omega)$ may be expanded in a power series in $1/\omega$ for large values of ω and that the coefficients are related to the number of possible walks on a lattice. The derivation is straightforward. By repeated use of the identity

$$1/(\omega - H') = 1/\omega + (1/\omega)H' [1/(\omega - H')] , \quad (2.5)$$

we can expand G , and we obtain the result for $|\omega| > zt$,

$$G_{ii}^{\alpha_i}(\omega) = \frac{1}{\omega} + \frac{1}{\omega} \sum_{p=2}^{\infty} \frac{A_p^{\alpha_i}}{z^p} \left(\frac{zt}{\omega}\right)^p , \quad (2.6)$$

where $A_p^{\alpha_i}$ is the total number of paths which start at site i with spin configuration α_i and return to the same site i with the same spin configuration α_i after exactly p steps.

The moments of the density of states M_l can be directly related to the coefficients A_p^{α} . Using the

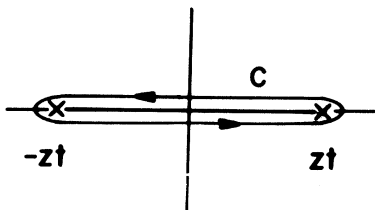


FIG. 1 Contour used in evaluating the moments of the density-of-states function.

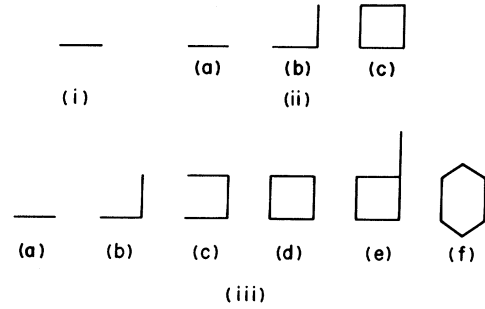


FIG. 2. Illustration of possible paths in (i) second order, (ii) fourth order, (iii) sixth order.

relation between the density of states per site $\rho^\alpha(\omega)$ and the imaginary part of the Green's function, we can write

$$M_l^\alpha = \int_{-zt}^{zt} \left(\frac{\omega}{zt}\right)^l \rho^\alpha(\omega) d\omega , \quad (2.7)$$

$$M_l^\alpha = \frac{1}{N} \sum_i \int_{-zt}^{zt} \left(\frac{\omega}{zt}\right)^l \text{Im}[G_{ii}^{\alpha_i}(\omega)] \frac{d\omega}{\pi} . \quad (2.8)$$

Now $G(\omega)$ is an analytic function of ω everywhere except for a cut on the real axis between $-zt$ and zt . Thus we may write the integral (2.8) as a contour integral around the cut

$$M_l^\alpha = \frac{1}{N} \sum_i \int_C \left(\frac{\omega}{zt}\right)^l G_{ii}^{\alpha_i}(\omega) \frac{d\omega}{2\pi i} , \quad (2.9)$$

where C denotes the contour shown in Fig. 1. Substituting the series (2.6) for G and deforming the contour to a circle of radius zt , we find the result

$$M_l^\alpha = A_l^\alpha / z^l . \quad (2.10)$$

It remains to calculate the coefficients A_l . This can be done by examining all possible paths and assigning a weight factor to each path depending on the spin configuration and calculating the weighted sum of all paths. It is convenient for this analysis to divide up the paths in each order according to the type of geometric figure described by the hole. Thus, in second order we have only one possible type of path, a walk to a nearest neighbor and immediate return, which is shown in Fig. 2(i). Since the spin of nearest neighbor is returned to its original position at the end of the walk, this path clearly has weight independent of the spin configuration. In fourth order there are three types of paths shown in Fig. 2(ii). For each type of configuration we calculate first, the lattice constant, or the number of ways it is possible to place the geometric figure on the lattice, second, the path factor or number of walks on such a geometric figure and third, the weight factor which depends on the spin configuration. The lattice

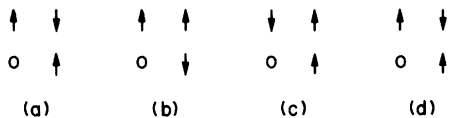


FIG. 3. Spin arrangements in the AF case which are obtained by successively walking around a square, (a) initial state, (b) after one revolution, (c) after two revolutions, and (d) after three revolutions.

constants and path factors for paths up to eighth order for a number of lattices have been tabulated by Domb.⁹ Thus, in fourth order the types (a), (b), (c) in Fig. 2(ii) have values of 3, 15, and 3, respectively, for the lattice constants and 2, 4, and 8 for the path factors. The total number of paths of $2l$ steps r_{2l} is given for the simple cubic lattice by

$$r_{2l} = \sum_{u,v,w} \frac{(2l)!}{(u!)^2(v!)^2(w!)^2}, \quad u+v+w=l. \quad (2.11)$$

In ferromagnetic spin configuration (F), all paths clearly have weight 1 and thus $A_l^F = r_l$. For the random-spin case (R) we examine the spin configuration at the end and assign a weight equal to $(\frac{1}{2})^{n-1}$ for each subgroup of n spins which must be aligned to make the path an allowed one. In the antiferromagnet (AF), we assign a weight 1 or 0 according to whether the final spin configuration is equal or not to the initial configuration. Applying these rules in fourth order, we assign weight 1 to the paths shown in Fig. 2(ii)(a) and 2(ii)(b), since the initial configuration is restored at the end of these walks. In fact, all paths which exactly retrace all the steps have weight 1 independent of the spin configuration. However, walks on a square, shown in Fig. 2(ii) (c), permute the initial spins. Thus, if we start with an antiferromagnetic spin configuration shown in Fig. 3(a) and walk on the square in an anticlockwise direction, we find the spins as shown in Fig. 3(b). Walks on a square, therefore, have a weight of $\frac{1}{4}$ (R) and 0 (AF) in fourth order. Note, however, that a walk on a square will contribute in twelfth order with weight 1, since, as shown in Fig. 3, the initial spin configuration is restored if the hole moves

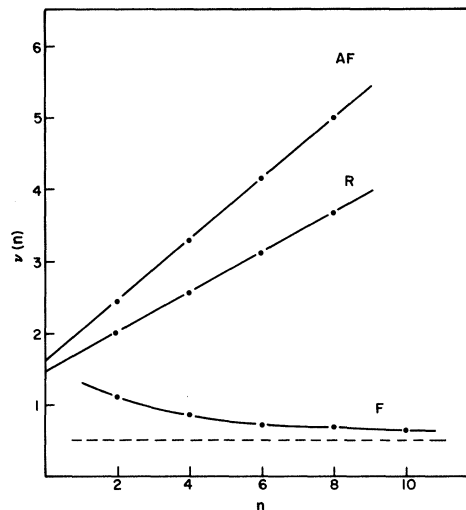


FIG. 4. Function $\nu(n)$ versus n .

around three times.

In this way we can evaluate the A_l in a straightforward manner. The algebra, however, expands rapidly with each order. In sixth order we find six types of path as shown in Fig. 2(iii). Following our rules we assign weight factors as follows: (a)–(c) have weight 1 for (R) and (AF), and (d) and (e) have weight $\frac{1}{4}$ (R) and 0 (AF), and (f) has weight $\frac{1}{16}$ (R) and 0 (AF). In Table I we tabulate the results we have obtained up to tenth order. We note that while, as pointed out previously by Harris and Lange,⁵ the first two moments M_0 and M_2 are independent of spin configuration, there are significant deviations in higher orders between the three spin configurations. The higher moments for the (R) and (AF) are substantially reduced suggesting a narrowing of the band.

From a knowledge of the moments M_n , we can determine in an approximate way the position and analytic form of the renormalized band edge. Thus, if we assume a simple-power-law singularity at the edge, of the form

$$\rho(\omega) = c \left[\omega_0^2 - \left(\frac{\omega}{zt} \right)^2 \right]^\nu, \quad |\omega/zt| < \omega_0 \\ = 0, \quad |\omega/zt| > \omega_0 \quad (2.12)$$

TABLE I. Number of weighted paths and the values of the moments.

l	A_l			M_l		
	F	R	AF	F	R	AF
2	6	6	6	0.166 67	0.166 67	0.166 667
4	90	72	66	0.069 44	0.055 56	0.050 926
6	1860	1 072 $\frac{1}{2}$	876	0.039 87	0.022 99	0.018 776
8	44 730	17 781 $\frac{3}{4}$	12 786	0.026 63	0.010 59	0.007 612
10	1 172 556	314 403	197 796	0.019 39	0.005 20	0.003 271

we can approximately determine ω_0^2 and ν from the exact M_n . Substituting the form (2.12) in Eq. (2.7) one can readily show that the ratio of succeeding moments M_n has the form

$$M_{n+2}/M_n = \omega_0^2(n+1)/(n+2\nu+3) . \quad (2.13)$$

This suggests that we write the ratio of the exact moments in the form

$$M_{n+2}/M_n = (n+1)/[n+2\nu(n)+3] , \quad (2.14)$$

or solving for $\nu(n)$ we find

$$\nu(n) = \frac{1}{2(M_{n+2}/M_n)} \left[n+1 - (n+3) \frac{M_{n+2}}{M_n} \right] . \quad (2.15)$$

In Fig. 4 we plot the function $\nu(n)$ determined by (2.15). This plot shows up in a dramatic way the difference between the different spin configurations. While for the ferromagnetic case $\nu(n)$ is clearly approaching its asymptotic value of $(\frac{1}{2})$, in the R and AF cases $\nu(n)$ appears to be increasing linearly with n . If we write $\nu(n) = an + b$, then from (2.13) we find that

$$\omega_0^2 = 1/(1+2a); \quad 2\nu = (2b+3)/(1+2a) - 3 . \quad (2.16)$$

From the intercepts and slopes of the straight lines in Fig. 4 we then arrive at the values of $\omega_0 = 0.805$ (R), $\omega_0 = 0.742$ (AF), $\nu = 0.40$ (R) and $\nu = 0.195$ (AF). These results suggest that for the R and AF the bulk of the band is narrowed by approximately 20 to 25%, respectively. These results differ considerably from the results found previously by different techniques. We shall return to this point below in Sec. II F.

We can also construct approximately the shape of the density of states for the whole band by ex-

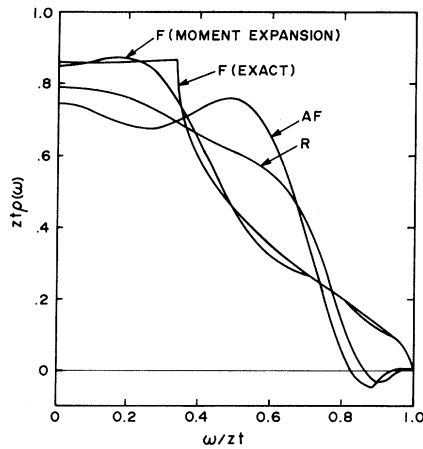


FIG. 5. Values of the density of states $\rho(\omega)$ given by the Legendre polynomial fit up to twelfth order for the spin configurations (F), (R), and (AF). For comparison the exact results for the case (F) are also shown.

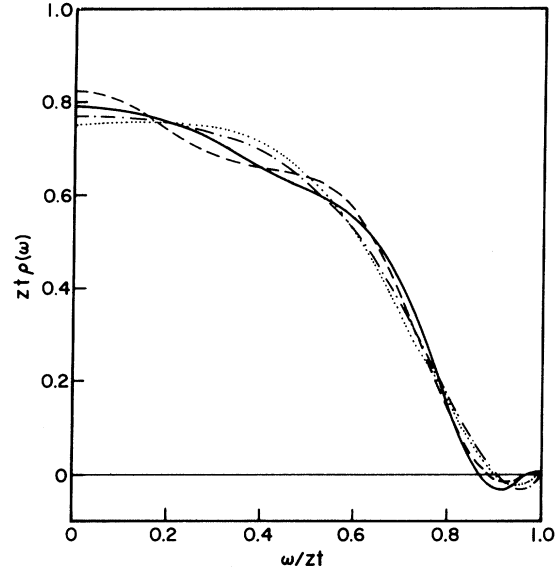


FIG. 6. Values obtained for $\rho(\omega)$ by truncating the Legendre polynomial fit at order 6 (dotted line), 8 (dot-dashed line), 10 (dashed line), and 12 (solid line) for the R case.

panding ρ in a series of Legendre polynomials whose coefficients are determined by the moments. Thus, if we write

$$zt\rho^\alpha(\omega) = \sum_{l=0}^{\infty} B_l^\alpha P_l\left(\frac{\omega}{zt}\right) \quad (2.17)$$

and substitute into Eq. (2.7), we find the following relation between the moments M_l^α and the Legendre coefficients B_l^α :

$$M_l^\alpha = \sum_{m=0}^l C(l,m) B_m^\alpha , \quad (2.18)$$

where $C(l,m) = \Gamma(\frac{1}{2}l + \frac{1}{2})\Gamma(\frac{1}{2}l + 1)/2\Gamma(\frac{1}{2}m + \frac{1}{2}l + \frac{3}{2}) \times \Gamma(\frac{1}{2}l - \frac{1}{2}m + 1)$. From the known moments, the B_m^α up to $m = 10$ are determined. We choose B_{12}^α so that $\rho(\pm zt) = 0$. In Fig. 5 we plot the values of $\rho^\alpha(\omega)$ obtained in this way as well as the exact results for the case F. The Legendre expansion to twelfth order for the F case gives a reasonably accurate representation of the exact band structure. In the R and AF cases the Legendre representation shows clearly the narrowing effect we discussed above. The over-all band shape appears to be rather flat at the center with a rapid drop off at the renormalized edges. The convergence of the Legendre polynomial expansion appears to be quite good. For example, in Fig. 6 we plot the values obtained for $\rho(\omega)$ by truncating Legendre polynomial fit at sixth, eighth, tenth, and twelfth order for the case (R). It is clear that the over-all shape we obtain does not vary much. Because of the finite number of Legendre polynomials used, there are

some unphysical oscillations in the shape. In particular, near $|\omega| = zt$ the curves go negative. In fact, as we shall discuss below, we believe that there is a band tail with a finite density of states stretching down to $\omega = zt$. However, it appears to be necessary to go to much higher order than tenth to obtain a significant contribution to the moments from the tail.

It is also of interest to represent $\rho^\alpha(\omega)$ as a series of Legendre polynomials within the range $|\omega| < \omega_0 zt$, where we use for the ω_0 , values determined above by considering the ratios M_n/M_{n+2} . Again we determine the $B_l^{\alpha'}$ for $l \leq 10$ from the moments and fix $B_{12}^{\alpha'}$ by demanding $\rho^\alpha(\pm \omega_0 zt) = 0$. The results obtained by this procedure are shown in Fig. 7. While there is some change in the detailed shape, the over-all conclusion for the body of the band is unchanged.

C. Walks with No Closed Loops

It is clearly desirable to have an approximate description for the states in the body of the band. If we examine the contributions to the moments which we have calculated, we find that the dominant contribution is from the class of walks in which the hole completely retraces all steps. These walks which involve no closed loops enter with weight 1. Domb⁹ refers to this class as walks with no closed configurations or walks on a Bethe lattice. This class is clearly not exact for the R configuration. For the AF configuration, however, the first correction to the moment expansion does not occur until twelfth order when the walk three times round the square becomes allowed. A comparison of A_l^R and A_l^{AF} for $l \leq 10$ from Table I shows that the graphs with weight 1 give the largest contribution to A_l^R also.

We can sum all walks with no closed loops and calculate the corresponding Green's function by using a technique similar to that used by Anderson in his paper on diffusion in random lattices.^{10,11} We first write the Green's function in terms of a self-energy

$$G_{ii}^{\alpha i}(\omega) = 1/\omega [1 - \Sigma_{ii}^{\alpha i}(\omega)] , \quad (2.19)$$

where $\Sigma_{ii}^{\alpha i}(\omega)$ is the sum of all graphs which do not have the original state $\{i\alpha_i\}$ as an intermediate state. In the remainder of this section we will suppress the superscripts α_i , since the class of walks we wish to consider do not depend on the spin configuration. The simplest approximation to the self-energy $\Sigma^{(1)}$ is a walk to the nearest neighbor and an immediate return shown in Fig. 2(i). Clearly,

$$\Sigma^{(1)}(\omega) = zt^2/\omega^2 . \quad (2.20)$$

Consider now the modification if we wish to include a walk in which we proceed from the nearest neighbor to one of its nearest neighbors. We can include this contribution by modifying the denominator in $\Sigma^{(1)}$ with a higher-order self-energy. The next approximation is, therefore,

$$\Sigma^{(2)} = \frac{zt^2}{\omega^2 [1 - (z-1)t^2/\omega^2]} . \quad (2.21)$$

The coefficient $(z-1)$ arises since we must include at the second step only forward going steps. We can now repeat this procedure, and by repeated application we generate a continued fraction for Σ :

$$\Sigma(\omega) = \frac{zt^2}{\omega^2 \left(1 - \frac{(z-1)t^2}{\omega^2 \left(1 - \frac{(z-1)t^2}{\omega^2 \left(1 - \frac{(z-1)t^2}{\omega^2 \dots} \right)} \right)} \right)} . \quad (2.22)$$

In this way all paths which completely retrace themselves, i. e., those with no closed loops, are summed. We can solve this continued fraction. If we write $\Sigma^A(\omega)$ for the sum of all forward going paths, then

$$\Sigma(\omega) = [z/(z-1)] \Sigma^A(\omega) , \quad (2.23)$$

and Σ^A satisfies the equation

$$\Sigma^A(\omega) = (z-1)t^2/\omega^2 [1 - \Sigma^A(\omega)] . \quad (2.24)$$

Equation (2.24) can be rewritten as a simple quadratic equation for Σ^A whose solution is

$$\Sigma^A(\omega) = \frac{1}{2} \pm \left[\frac{1}{4} - (z-1)t^2/\omega^2 \right]^{1/2} . \quad (2.25)$$

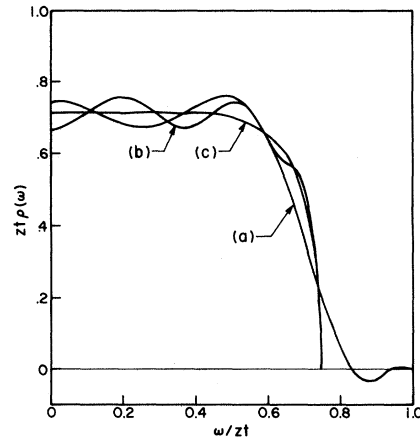


FIG. 7. Density of states obtained by (a) AF case Legendre polynomial expansion to twelfth order, (b) AF case, Legendre polynomial expansion in restricted region, and (c) from the sum of all walks with no closed loops.

Substituting in (2.23) and (2.19) we find

$$G(\omega) = \omega^{-1} \left\{ 1 - \frac{z}{(z-1)} \left[\frac{1}{2} - \left(\frac{1}{4} - \frac{(z-1)t^2}{\omega^2} \right)^{1/2} \right] \right\}^{-1}, \quad (2.26)$$

where we take negative root for Σ^A so that $G(\omega)$ has the correct limiting behavior as $\omega \rightarrow \infty$. The Green's function $G(\omega)$ is purely real for $|\omega| > 2(z-1)^{1/2}t$. For $z=6$, this gives a value for the edge of $\omega_0 = 0.745$. Using the relation between the density of states and the imaginary part of G we find

$$zt\rho(u) = (1/\pi)[(5-9u^2)^{1/2}/(1-u^2)], \quad u = \omega/zt. \quad (2.27)$$

In Fig. 7 we show the resulting curve for ρ . The density of states is very flat with a sharp square root singularity at the edge. Comparing with the Legendre fit based on the moment expansion results, we find good agreement, especially for the AF case. In the R case the agreement is less good, as one expects. Nonetheless, it is clear that by summing all walks with no closed loops we obtain a reasonably accurate representation of the body of the band. We do not obtain any band tails, and we shall return to this point in Sec. II E.

D. One Dimension

In this section, we digress somewhat from our main presentation to discuss, in detail, the problem in one dimension. This problem has been solved exactly by Lieb and Wu.¹² In fact, since there can be no walks on squares or other closed loops, the procedure we used in Sec. II D is exact in one dimension. Substituting the value $z=2$ in Eq. (2.26) we find the diagonal Green's function has the form

$$G_{ii}(\omega) = 1/(\omega^2 - 4t^2)^{1/2}, \quad (2.28)$$

independent of the spin configuration. Thus, the density of states in one dimension is just that for a single particle moving in the band. Various Green's-function decoupling schemes, however, lead to incorrect predictions that the band will be narrowed in one dimension.¹³

The reason for the simple result in one dimension can be seen by examining the structure of the Hamiltonian. Consider N sites on a ring with the hole initially at site i and spin configuration α_i . Then by repeatedly applying the Hamiltonian H' , we may move the hole around the ring. If we move the hole around the ring once, we have a different spin configuration except for the special case of ferromagnetic ordering. However, if we move the hole around $N-1$ times, then we arrive back at the same spin configuration we started with. Thus, in the space of the states $\Psi_{i\alpha_i}$, the matrix representa-

tion of H' is

$$H' = t \begin{bmatrix} 0 & 1 & 0 & 0 & 1 \\ 1 & 0 & 1 & & \\ 0 & 1 & 0 & 1 & 0 \\ & 0 & & 1 & 0 & 1 \\ 1 & & & & 1 & 0 \end{bmatrix} \quad (2.29)$$

The matrix has sides $N(N-1) \times N(N-1)$. However, apart from a different size, the structure is the same as in the ferromagnetic or single-particle case. Thus, the density of states is the same for all spin configurations.

While the density of states is the same as that of a single particle, the nature of the eigenfunctions is clearly very different. For a general spin configuration the eigenstates will be linear combinations of the $\Psi_{i\alpha_i}$ for $i=1 \cdots N$ and the $N-1$ distinct values of α_i for each i . These eigenstates are clearly true many-body states. They do, however, share one important property with the single-particle states. They are also eigenstates of the current operator. This can be seen by commutation of the current operator with H' . The current operator J may be written as

$$J = eati \sum_{j\sigma} c_{j+1,\sigma}^\dagger c_{j\sigma} - c_{j-1,\sigma}^\dagger c_{j,\sigma}, \quad (2.30)$$

where a is the lattice parameter. It is straightforward to show that in one dimension

$$[PJP, H'] = 0. \quad (2.31)$$

Therefore, all eigenstates of H' are eigenstates of the current operator.

The many-body nature of the eigenstates shows up clearly if we examine the off-diagonal components of the Green's function. Consider an antiferromagnetic spin configuration. Then it is straightforward to show that

$$G_{ij}^{AF}(\omega) = 0, \quad i \neq j. \quad (2.32)$$

The argument proceeds as follows. Using the definition we may write

$$G_{ij}^{AF}(\omega) = \left\langle \Psi_j^{AF} \left| \frac{1}{\omega - H'} \right| \Psi_i^{AF} \right\rangle. \quad (2.33)$$

Clearly, since H' conserves spin, only even values of $(i-j)$ can be nonzero. Consider a specific value of $j-i=4$. Then the states Ψ_i^{AF} and Ψ_j^{AF} are as shown in Figs. 8(a) and 8(b), respectively. The question now arises whether by repeatedly applying the Hamiltonian operator H' we can find a matrix element to link these two states. If we move the hole from i to j , the resulting state has the form shown in Fig. 8(c). Clearly, this state is not Ψ_j^{AF} . The argument can immediately be generalized to walks where the hole takes n steps

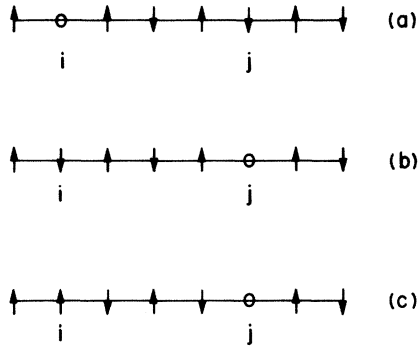


FIG. 8. Illustration of the states (a) Ψ_i^{AF} , (b) Ψ_j^{AF} , and (c) the state obtained by moving the hole from i to j .

in the positive direction and $n-4$ steps in the negative direction. The argument also does not depend on our choice $j-i=4$ and is quite general for all $j \neq 1$. Since $G_{ij}^{\text{AF}}(\omega)$ is a δ function in real space if we transform to reciprocal space we get at once

$$G^{\text{AF}}(\vec{k}, \omega) = 1/(\omega^2 - 4t^2)^{1/2} \quad (2.34)$$

This structure is very different from that of a single-particle Green's function

$$G^{\text{F}}(\vec{k}, \omega) = 1/(\omega - 2t \cos ka) \quad (2.35)$$

Thus, one cannot give a quasiparticle description, i. e., single-particle propagation with weak damping, of G^{AF} . This stresses again the essential many-body aspect of the problem.

Similar results are found for the random configuration. We start with a given random-spin arrangement and study the states Ψ_i^{R} and Ψ_j^{R} which arise if we annihilate a down spin, say at sites i and j , respectively, for this given configuration. We now apply the argument given above for the AF case. The argument still applies except for the configurations in which all the spins from i to j inclusive are aligned in the same direction. For such a configuration, clearly, $G_{ij} \equiv G_{ij}^{\text{F}}$. Averaging over all possible random configurations we arrive at the result

$$G_{ij}^{\text{R}}(\omega) = (\frac{1}{2})^{|i-j|} G_{ij}^{\text{F}}(\omega) \quad (2.36)$$

Taking the Fourier transform, we find

$$G^{\text{R}}(k, \omega) = \sum_{k'} \frac{1}{\omega - 2t \cos k'a} \times \sum_{n=0}^{\infty} (\frac{1}{2})^n (e^{ina(k-k')} + e^{-ina(k-k')}) \quad (2.37)$$

$$G^{\text{R}}(k, \omega) = \sum_{k'} \frac{1}{\omega - 2t \cos k'a} \left(\frac{1}{1 - \frac{1}{2} e^{ia(k-k')}} + \text{c. c.} \right) \quad (2.38)$$

Let us examine the imaginary part of G^{R} . In the quasiparticle description, $\text{Im}G$ should be a sharply peaked function. However, from (2.38) one finds

$$\text{Im}G^{\text{R}}(k, \omega) = \pi\rho(\omega) \times \left(\frac{2 - \cos(k-k_0)a}{5 - 4 \cos(k-k_0)a} + \frac{2 - \cos(k+k_0)a}{5 - 4 \cos(k+k_0)a} \right), \quad (2.39)$$

$$k_0 a = \cos^{-1}(\omega/2t) \quad .$$

The function in the large parenthesis is a slowly varying one whose maximum value is 2, so that the G^{R} does not have the form of a single Lorentzian peak which is characteristic of a quasiparticle picture.

E. Band Tails

So far, the approximations we have discussed have led to bands which are narrowed by approximately 20–25% and have sharp edges at $\omega = \pm \omega_0 zt$. Nagaoka⁶ has shown that the ground state for an extra electron or hole is the uniform ($k=0$) state with ferromagnetic alignment of the spins. The uniform hole state has an energy $\omega = -zt$. The question immediately arises as to whether there are states in the region $\omega_0 zt \leq |\omega| \leq zt$. In this section we will examine this question and present arguments which lead us to believe that there will be such states and that in the true band there will be tails stretching to $|\omega| = zt$.

The important paths which we have to consider here are those in which the hole walks and rewalks over a limited number of sites. It is interesting to ask how large a cluster is needed to obtain a state below the edge at $\omega = -\omega_0 zt$. One can include, in addition to all possible walks on the central cluster, all paths which are completely self-retracing and which start from the corners of the central cluster without reducing the weight on the state. It is straightforward but rather tedious to perform such calculations, and we shall merely state the results. One finds that a central cluster of twelve sites arranged on a solid rectangle is required to obtain a bound state just very slightly below the edge. The weight in this state is very small, 1/2048 (R) and 1/5548 (AF), respectively.

Clearly, as we expand the size of the central cluster, the bound state will move to lower energies until, by making the size of the central cluster as large as we like, we can approach as close as we like to the edge of the ferromagnetic band at $\omega = zt$. However, the larger the central cluster, the smaller the weight contributed by the bound state. We can use the argument given by Lifshitz¹⁴ for the form of an impurity band tail to give us an approximate form for the density of states in the tail. Consider first the random case. The probability

that a cluster of M states is ferromagnetically aligned is $(2M+1)2^{-M}$. The lowest state in such a configuration will have energy measured from the bottom of the ferromagnetic band

$$\omega + zt = t x_0 M^{-2/3}, \quad x_0 = \left(\frac{4}{3}\right)^{2/3} \pi^{8/3}. \quad (2.40)$$

In writing (2.40) we take only spherical clusters. Solving for M in terms of $(\omega + zt)$ we find the density of states, assuming that each cluster of M spins contributes one state

$$\rho^R(\omega) \sim \left(\frac{t}{\omega + zt}\right)^{3/2} e^{-\lambda/(\omega + zt)^{3/2}}, \quad \lambda = \frac{4}{3} \pi^4 t^{3/2} \ln 2. \quad (2.41)$$

The constant λ is only approximate as, for example, large ferromagnetic clusters which are far from spherical can contribute terms of the same form. We can also apply similar arguments to the AF case. Here we must use for the probability factor the projection of the up-down alignment for a cluster of M sites on the ferromagnetic state. This projection has the asymptotic form

$$\frac{(\frac{1}{2}M)!}{M!} \xrightarrow{M \rightarrow \infty} \exp(-M \ln 2 - \frac{1}{2} \ln M). \quad (2.42)$$

This leads to a form for the density of states

$$\rho^{AF}(\omega) \sim \left(\frac{\omega + zt}{t}\right)^{3/4} e^{-\lambda/(\omega + zt)^{3/2}}. \quad (2.43)$$

The existence of band tails in this model raises several interesting questions. First, will these states in the tail carry a current or will they be localized in the Anderson¹⁰ sense? Second, does the edge of the narrowed band that we find correspond to a real singularity in the density of states? We do not have a complete answer to either question. Although we derived the existence of tails by arguments similar to those used for impurity band tails, there are important differences between the two situations. In the AF case, the system has translational invariance so that there is no fixed constraint to force the wave function to zero over most of the crystal. Similarly, for the random case the motion of hole itself can change the spin configuration unlike a configuration of fixed impurities. These considerations lead us to believe that these states will carry a current. However, undoubtedly these states will have extremely low mobility. In a sense these states can be thought of as large magnetic polarons. This also suggests that the edge which we find at $\omega_0 zt$ will not be a true singularity, but only a region of rapid variation of the mobility and the density of states.

F. Comparison to Other Treatments of the Hubbard Model

It is of interest to compare this composite pic-

ture, in which the bulk of the band is narrowed by 20–25% depending on the spin configuration and in which there are band tails stretching to $\pm zt$, with the results obtained by other approaches. In his original papers on this problem, Hubbard⁴ used a Green's-function decoupling scheme. He limited his attention, however, to random-spin configurations. In his first paper, his approximation for the band shape was similar to the mean field approach to the alloy problem. He found a band which was narrowed over all by a factor of $\frac{1}{2}$. In his third paper, Hubbard presented an improved version of the decoupling scheme which led to density of states with the full bandwidth without band tails in the atomic limits. Subsequently, various authors have considered other decoupling schemes.

An alternative approach has been given by Bulaevskii and Khomskii.¹⁵ These authors have started in the atomic limit by taking the interaction term in the Hamiltonian (2.1) as the unperturbed Hamiltonian and used the hopping term as a perturbation. They consider both the AF and R configurations. Their results lead to a bandwidth which is strongly dependent on spin configuration. Thus, they find a bandwidth for the AF case of

$$\Omega_b = 2zt \left(\frac{\frac{1}{4} + \langle S_{\mathbf{i}} \cdot S_{\mathbf{i}+\mathbf{n}} \rangle}{(\frac{1}{4} - S_0^2)^{1/2}} \right) + O\left(\frac{t^2}{U}\right), \quad (2.44)$$

where $\langle S_{\mathbf{i}} \cdot S_{\mathbf{i}+\mathbf{n}} \rangle$ is the expectation value of the scalar product of the spin operators on nearest-neighbor sites, and S_0 is the sublattice magnetization. Thus at $T = 0$ °K, one finds a bandwidth which is proportional to the zero-point deviation. At temperatures much higher than the Néel temperature when the spin configuration is random, $\langle S_{\mathbf{i}} \cdot S_{\mathbf{i}+\mathbf{n}} \rangle = \frac{1}{2}$, and one finds the result of Hubbard's first paper.⁴ There is a large change in bandwidth with spin configuration in contrast to the rather small changes which we have found in this section.

III. CALCULATION OF MOBILITY

Within the approximation that the dominant paths for the motion of the hole are those with no closed loops, we can calculate the mobility of a hole. The picture that emerges from this calculation is that the hole essentially undergoes a Brownian motion because of the strong scattering due to the non-ferromagnetic arrangement of the spins. The scattering of the hole is elastic in the limit $t/U = 0$, since all spin waves have zero energy. The results will therefore be unphysical within a characteristic spin-flip energy of the band edge. The results should therefore be valid at temperatures well above the ordering temperature. In the AF phase, our approximation will apply only to carriers whose

energy, measured from the renormalized band edge, is much larger than the exchange energy.

In order to calculate the mobility, we start with the Kubo formula for the conductivity¹⁶

$$\sigma = \frac{1}{Z\Omega} \int_0^\infty dt \int_0^\beta d\lambda \text{Tr} \left(\rho_0 J_x e^{iH'(\tau+i\lambda)} J_x e^{-iH'(\tau+i\lambda)} \right). \quad (3.1)$$

In this expression the trace is to be taken over all states with a single hole and arbitrary spin configurations. ρ_0 is the density operator $e^{-\beta H'}$, Ω is the volume of the system, Z is the partition function for a single hole, and $\beta = 1/k_B T$. The tight-binding expression for the current operator for the simple cubic band is

$$J_x = e \sum_{k,\sigma} \frac{d\epsilon_k}{dk_x} c_{k\sigma}^\dagger c_{k\sigma}, \quad (3.2)$$

$$J_x = e a t i \sum_{i\sigma} (c_{i+x\sigma}^\dagger c_{i\sigma} - c_{i-x\sigma}^\dagger c_{i\sigma}), \quad (3.3)$$

where $(i+x)$ is the lattice site next to i in the positive x direction. By inserting resolvent representations of the two exponential operators and doing the τ and λ integrals, we arrive at the result that

$$\sigma = \frac{(-1)}{Z\Omega} \int_{-zt}^{zt} \frac{d\omega_1 d\omega_2}{4\pi} \delta(\omega_1 - \omega_2) \times [(e^{-\beta\omega_2} - e^{-\beta\omega_1}) / (\omega_1 - \omega_2)] F(\omega_1, \omega_2), \quad (3.4)$$

$$\sigma = \frac{-\beta}{Z\Omega} \int_{-zt}^{zt} \frac{d\omega_1}{4\pi} e^{-\beta\omega_1} F(\omega_1, \omega_1). \quad (3.5)$$

Here

$$F(\omega_1, \omega_2) = \mathfrak{F}(\omega_1 + i\delta, \omega_2 + i\delta) + \mathfrak{F}(\omega_1 - i\delta, \omega_2 - i\delta) - \mathfrak{F}(\omega_1 + i\delta, \omega_2 - i\delta) - \mathfrak{F}(\omega_1 - i\delta, \omega_2 + i\delta), \quad (3.6)$$

where

$$\mathfrak{F}(\omega_1, \omega_2) = \text{Tr} [(\omega_1 - H')^{-1} J_x (\omega_2 - H')^{-1} J_x], \quad (3.7)$$

$\mathfrak{F}(\omega_1, \omega_2)$,

$$= 2e^2 a^2 t^2 \sum_{i\sigma, j\sigma'} \text{Tr} \left(\frac{1}{\omega_1 - H'} c_{i-x\sigma}^\dagger c_{i\sigma} \frac{1}{\omega_2 - H'} c_{j+x\sigma'}^\dagger c_{j\sigma'} - \frac{1}{\omega_1 - H'} c_{i+x\sigma}^\dagger c_{i\sigma} \frac{1}{\omega_2 - H'} c_{j-x\sigma'}^\dagger c_{j\sigma'} \right). \quad (3.8)$$

We consider the lowest-order approximation to this expression and later show that the higher-order corrections are not large and do not change the physical interpretation. The lowest-order approximation is that in which only the $i=j+x$ term in (3.8) is kept. Then

$$\mathfrak{F}^0(\omega_1, \omega_2) = 2e^2 a^2 t^2 G(\omega_1) G(\omega_2). \quad (3.9)$$

Inserting this expression into (3.5) and (3.6), we have

$$F^0(\omega_1, \omega_1) = -8e^2 a^2 t^2 [\text{Im}G(\omega_1)]^2, \quad (3.10)$$

and defining the mobility of the hole as

$$\begin{aligned} \mu &= \sigma \Omega / e \\ &= 2\beta e a^2 t^2 \int_{-zt}^{zt} \frac{d\omega}{\pi} e^{-\beta\omega} [\text{Im}G(\omega - i\delta)]^2 / \int_{-zt}^{zt} \frac{d\omega'}{\pi} e^{-\beta\omega'} \\ &\quad \times \text{Im}G(\omega' - i\delta). \end{aligned} \quad (3.11)$$

Within this approximation the mobility is proportional to the average over the thermally occupied states of the hopping probability $zt^2 \text{Im}G(\omega - i\delta)$. The $\text{Im}G(\omega - i\delta)$ simply measures the density of states at the neighboring site. To obtain some typical values of the mobility, we substitute (2.26) for G , and we have

$$\text{Im}G(\omega - i\delta) = \frac{1}{2} z [(\omega_0 z t)^2 - \omega^2]^{1/2} / [(z t)^2 - \omega^2], \quad (3.12)$$

$$\text{Im}G(\omega - i\delta) \simeq (\frac{1}{2} \omega_0)^{1/2} \frac{z}{(z t)^{3/2}} \frac{(\omega_0 z t + \omega)^{1/2}}{(1 - \omega_0^2)}, \quad (3.13)$$

for $\omega \approx \omega_0 z t$. Inserting this expression into (3.11), we find for $k_B T \ll z t$ that

$$\begin{aligned} \mu &= [e a^2 4z / (z - 2)^2] [2(z - 1) / \pi] \beta t^{1/2} \\ &\quad \times [2(z - 1)^{1/2} \beta t / \pi]^{1/2}; \end{aligned} \quad (3.14)$$

if $(\beta z t) = 100$ and $a = 3 \text{ \AA}$, this gives $\mu = 7.1 \text{ cm}^2/\text{V sec}$. If we take $k_B T > z t$, we can perform the integrals in (3.11) to obtain

$$\begin{aligned} \mu &= \frac{\beta e a^2 z t}{\pi} \left[\frac{(\omega_0^2 - 1)}{2} \ln \left(\frac{1 + \omega_0}{1 - \omega_0} \right) + \omega_0 \right] \\ &= (\beta z t) \times 0.14 \text{ cm}^2/\text{V sec}. \end{aligned} \quad (3.15)$$

These values of the mobilities are relatively small even when the bandwidth is of the order of 1 eV. The reason for this low mobility is that the hole is essentially undergoing Brownian motion through the lattice.¹⁷ Although we have underestimated somewhat the mobility due to the limited paths we have considered, especially in the random case, it is clear that one cannot treat the bands in magnetic insulators as freely propagating with weak scattering. It is customary to ascribe the low mobility in transition-metal oxides to polaron formation. Although corrections of order t^2/U must be included before any comparison with experiment can be made, we note that the mobilities calculated here without polaron effects are of the same order of magnitude as the experimentally measured mobilities in, for example, NiO^3 at high temperatures.

We now discuss the corrections to (3.9) for $i \neq j + x$. Substituting the expansion (2.5) for $(\omega_1 - H')^{-1}$ into (3.8), the \mathfrak{F} function is written in terms

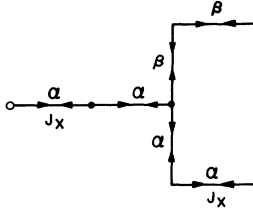


FIG. 9. Illustration of the type of paths summed in calculating the mobility. The steps labeled α make up an irreducible path and those labeled β , a side excursion.

of paths in which the hole first takes a step with the current operator, then m steps with the operator (H'/ω_2) , then a step with the second current operator and finally m' steps with the operator (H'/ω_1) . Only paths where the hole returns to its original position and the spin configuration is left unchanged contribute. We work with the approximation in which only those paths which contain no closed loops are included. These are conveniently classified according to the number of steps taken using (H'/ω_2) which are not retraced before the second J_x operates. Suppose there are n of these. These n steps necessarily form a forward going path, i. e., a path with no immediate reversals. Such an n -step path is an irreducible path to which any number of vertex renormalizations or side excursions may be added. This is illustrated in Fig. 9. The steps labeled α in this figure form a possible irreducible path, while those labeled β form one possible side excursion. The J_x symbols on the ends of the α path indicate that one of the steps at that point is taken with the current operator. Before the first step along the irreducible path is taken, the hole can make arbitrary excursions, always eventually returning to the first site. This gives a contribution $G(\omega_2)$. After the first step, the hole can again take arbitrary excursions, provided it does not immediately return to the first site. Such forward-going excursions were summed in Sec. II to give $[1 - \Sigma^A(\omega_2)]^{-1}$. This can be done after any of the n steps along the irreducible path. After operating with the second J_x operators, the return path is completely determined, except for side excursions. These excursions can be summed in the same fashion as those for the (H'/ω_2) operator. Therefore, from the sum of all n th order irreducible paths, we obtain a contribution to μ of the form

$$2e^2 a^2 t^2 G(\omega_1) G(\omega_2) \left(\frac{t}{\omega_2 [1 - \Sigma^A(\omega_2)]} \right)^n \times \left\{ \frac{A_n t^{n-2}}{\{\omega_1 [1 - \Sigma^A(\omega_1)]\}^{n-2}} + \frac{B_n t^n}{\{\omega_1 [1 - \Sigma^A(\omega_1)]\}^n} \right\}$$

$$+ \frac{C_n t^{n+2}}{\{\omega_1 [1 - \Sigma^A(\omega_1)]\}^{n+2}}, \quad (n \geq 2) \quad (3.16)$$

where A_n is the number of paths in which both steps taken with the J_x 's are retraced by the (H'/ω_2) operator, B_n is the number in which one of the J_x steps is retraced by (H'/ω_2) , and finally, C_n is the number of paths in which neither J_x operator is retraced by (H'/ω_2) -type steps. In calculating these coefficients there is a large cancellation between the two terms in (3.8). First, consider all paths in which the last step taken with (H'/ω_2) is not along $\pm x$. When the step taken using the second current operator is added, the return path is the same length for both directions of this step. Therefore, the two paths give equal and canceling contributions to the difference in (3.8). Next, consider these paths whose last l steps before the second J_x operator are along the positive x axis $0 < l < n$. If the step taken using the first current operator was retraced by the first step taken using (H'/ω_2) , such a path gives a +1 contribution to A_n and a -1 contribution to B_n . If the first step is not retraced immediately, such a path gives a +1 to B_n and a -1 contribution to C_n . In either case, the path which is identical with the above path, except that its last l steps are in the $-x$ direction instead of the $+x$ direction, gives a contribution which exactly cancels the contribution from the original path. Figure 10 illustrates this cancellation. Path (a) gives a +1 contribution to A_n , while path (b) gives a -1 contribution to A_n so that they cancel identically in the calculation of the current. Therefore, the only paths left are those with all n steps in the positive or negative x direction. These two paths give $A_n = -1$, $B_n = 2$, and $C_n = -1$ for $n \geq 2$. Since $A_1 = 0$, $B_1 = 1$, and $C_1 = -1$, we can sum the series to obtain

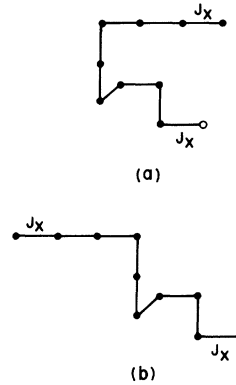


FIG. 10. Two irreducible graphs whose contributions to the current cancel. The starting site is indicated by the circle, and the J_x indicates the steps taken using the current operations.

$$\mathcal{F}(\omega_1, \omega_2) = 2e^2 a^2 t^2 G(\omega_1) G(\omega_2) [1 + 1/\alpha_1 \alpha_2 - (\alpha_1^2 + \alpha_2^2 - 2)/\alpha_1 \alpha_2 (\alpha_1 \alpha_2 - 1)] , \quad (3.17)$$

where

$$\alpha_1 = \omega_1 t^{-1} [1 - \Sigma^A(\omega_1)]$$

and

$$\alpha_2 = \omega_2 t^{-1} [1 - \Sigma^A(\omega_2)] .$$

The cancellation of the contributions from all paths but those along the x axis has led us to an expansion in powers of $(\alpha_1 \alpha_2)^{-1}$. For $\omega_1 = \omega_2$,

$$|(\alpha_1 \alpha_2)^{-1}| = (z - 1)^{-1} , \quad (3.18)$$

so that the higher-order terms give only a small correction for the simple cubic lattice where $z = 6$. To make explicit the size of the corrections to the mobility, we define

$$v^2(\omega_1) = F(\omega_1, \omega_1) / F^0(\omega_1, \omega_1) , \quad (3.19)$$

so that

$$\mu = 2\beta e a^2 t^2 \int_{-zt}^{zt} \frac{d\omega}{\pi} e^{-\beta\omega} [\text{Im}G(\omega - i\delta)]^2 v^2(\omega_1) \Big|$$

$$\int_{-zt}^{zt} \frac{d\omega'}{\pi} e^{-\beta\omega'} \text{Im}G(\omega' - i\delta) . \quad (3.20)$$

The $v^2(\omega_1)$ is the correction to (3.11) due to the higher-order terms. After some algebra we find that

$$v^2(\omega_1) = \frac{z}{(z-2)} \left[1 - \frac{4(2z-3)}{z^2(z-1)} \left(\frac{\omega_1}{\omega_0 z t} \right)^2 \right] . \quad (3.21)$$

This function varies by 20% over the band ($z = 6$), so that the higher-order terms change the mobility by roughly $z/(z-2)$ ($= 1.5$).

In one dimension the above sum includes all paths and is therefore exact. In this case $v^2 = \infty$, and the mobility is infinite in accordance with the discussion in Sec. II.

IV. INCLUSION OF t/U TERMS AND INTRA-ATOMIC EXCHANGE

A. Corrections of Order t/U

In the previous sections we have been discussing the extreme atomic limit where no doubly occupied atomic sites are allowed. The first-order corrections to these results of order t/U are due to the admixture of states with one doubly occupied site. This admixture would be a small effect if it were not for the fact that it gives rise to an indirect coupling between the degenerate states with energies of order zero with respect to U . The mixing of these states has nontrivial effects on some of the properties of the spectral functions calcu-

lated in Sec. II. In particular, the tails will be changed considerably. In order to discuss the effect of these terms, we again consider a Hamiltonian projected onto the subspace of states with singly occupied atoms, but which includes the effects of virtual transitions to doubly occupied states. This Hamiltonian was discussed by Harris and Lange,⁵ and it can be written in the form

$$H' = \sum_{ij} t_{ij} c_{i\sigma}^\dagger c_{j\sigma} - \sum_{ijl} \frac{t_{il} t_{lj}}{U} c_{i\sigma}^\dagger (1 - n_{l\sigma}) c_{j\sigma} + \sum_{i,j} \frac{2t_{ij}^2}{U} (\vec{S}_i \cdot \vec{S}_j - \frac{1}{4} \rho_i \rho_j) . \quad (4.1)$$

Here

$$\vec{S}_i = \frac{1}{2} \sum_{\sigma\sigma'} \vec{\sigma}_{\sigma\sigma'} c_{i\sigma}^\dagger c_{i\sigma'} , \quad (4.2)$$

$\vec{\sigma}$ being the Pauli matrices, and

$$\rho_i = \sum_{\sigma} c_{i\sigma}^\dagger c_{i\sigma} . \quad (4.3)$$

There will, in general, be considerable cancellation between the last two terms in the determination of the over-all width of the band, since the second term represents a propagation effect, while the third term tends to inhibit the hopping described by t_{ij} . However, the states in the tail of the band are those in which the hole is propagating in a ferromagnetic region of the crystal. To the extent that this is true, we can ignore the second term in (4.1) in considering these states. For the random configuration or for $k_B T \gg t^2/U$, the probability distribution for finding large ferromagnetic regions is the same as with $t/U = 0$ and, therefore, the tails extend to at least $\omega = \pm zt$. In the AF case the situation is similar to that for double exchange discussed by De Gennes¹⁸ and applied to the present problem by Herring.¹⁹ Assume the hole is confined to a region containing N atoms so that its total kinetic energy is (the region is taken to be a cube and the wave function a product of cosines)

$$E_k \simeq -zt \cos\left(\frac{\pi}{N^{1/3} + 1}\right) \simeq -zt + \frac{z\pi^2 t}{2N^{2/3}} . \quad (4.4)$$

The hole can have this value of kinetic energy only if all the spins in this region are aligned ferromagnetically. This costs an energy

$$N z t^2 / U . \quad (4.5)$$

Minimizing the sum of these terms with respect to N , we find a minimum energy of (assuming $N \gg 1$)

$$E_m = -zt + \frac{5}{3} (2\pi^2)^{3/5} t (zt/U)^{2/5} , \quad (4.6)$$

with the number of atoms involved being

$$N = (U/zt)^{3/5} (2\pi^2)^{3/5} . \quad (4.7)$$

Thus, the extent of the tails will be reduced owing

to the energy required to create large ferromagnetic regions. Within this approximate calculation, we can estimate when this effect is strong enough to eliminate the tails completely. This is roughly when $\frac{5}{3}(2\pi^2)^{3/5}t(zt/U)^{2/5} = \frac{1}{4}zt$, i. e., when the binding energy in the ferromagnetic region is equal to the band edge calculated from (2.26). This gives $(zt/U) \approx 0.01$, a very small value. The correct answer is undoubtedly considerably larger because energy can be gained by tilting the spins slightly and not requiring them to be perfectly ferromagnetic. It should also be noted that (4.4) is only a crude estimate of the energy gained in a ferromagnetic region. For example, in Sec. II we discussed a calculation on only twelve atoms which gave a state below the continuum edge. Such a twelve-atom state is not possible according to (4.4). Physically, one expects these "spin polaron" states to exist out to quite reasonable values of zt/U .

In contrast to the tails, the bulk of the spectral function does not seem to change appreciably owing to t^2/U corrections. This can be judged by examining the corrections to the first few moments. These moments are somewhat more complicated to calculate, and we follow the methods of Harris and Lange. The n th moment of the density of states for a hole at i of spin σ is

$$M_{i\sigma}^n = \langle c_{i\sigma}^\dagger [\dots [c_{i\sigma}, H'], H'] \dots]_n \rangle / \langle c_{i\sigma}^\dagger c_{i\sigma} \rangle . \quad (4.8)$$

We have normalized these so that the total spectral weight is one. It is not difficult to see that the first-order corrections to the even moments in t/U are zero, since one cannot take an odd number of steps with the direct t_{ij} operator and return to the origin with any of the other operators in (4.1). Using (4.1) we find

$$\begin{aligned} M_{i\sigma}^1 &= -zt^2/U, & \text{R} \\ &= -2zt^2/U, & \text{AF} . \end{aligned} \quad (4.9)$$

These are simply shifts in the center of the spectral function. We measure the higher moments from this shifted center. We have again taken the AF configuration to be simply the up-down configuration and have not included zero-point deviations:

$$\begin{aligned} M_{i\sigma}^3 &= -30t^4/U, & \text{R} \\ &= 0, & \text{AF} . \end{aligned} \quad (4.10)$$

Thus, to lowest order, the major change in the spectral function is a small shift of center, due to the fact that it now costs energy to remove a particle at a site, and an asymmetry, due to the additional means of propagating the hole through the crystal for the R configuration. Neither of these effects appear to be strong effects on the bulk of the band.

B. Intra-Atomic Exchange

If one considers a more realistic situation there will be more than one band, and intra-atomic exchange becomes important. The modified form of the Hamiltonian incorporating this effect²⁰ is

$$\begin{aligned} H &= \sum_{ij} \sum_{mm';\sigma} t_{ij}^{mm'} c_{im\sigma}^\dagger c_{jm'\sigma} \\ &+ \frac{1}{2}U \sum_{mm';i;\sigma\sigma'} c_{im\sigma}^\dagger c_{im'\sigma'}^\dagger c_{im'\sigma'} c_{im\sigma} \\ &+ \frac{1}{2}J \sum_{mm';i;\sigma\sigma'} c_{im\sigma}^\dagger c_{im'\sigma'}^\dagger c_{im'\sigma'} c_{im\sigma} . \end{aligned} \quad (4.11)$$

Here J is the intra-atomic exchange integral, and m labels the various degenerate states of the atom. To illustrate the effect of intra-atomic exchange, suppose the hopping integral is diagonal in m and $J \gg |t_{ij}^m|$. We again work in the atomic limit $t/U \rightarrow 0$ and consider two electrons per atom. A generalization to higher numbers is straightforward. The two electrons on each site are coupled according to Hund's rule into triplet states. A hole on one site can hop to a neighbor no matter which of the three spin states the neighbor is in before the hop. The matrix elements depend on the spin state of the neighbor and the spin of the electron on the site of the hole. If we designate the initial atomic state of the two sites involved in the hop by $|\pm 1/2, m\rangle$, $m = \pm 1, 0$ and the final state after the hop by $\langle m, \pm 1/2|$, then

$$\begin{aligned} \langle 1, \frac{1}{2} | H' | \frac{1}{2}, 1 \rangle &= t , \\ \langle 1, -\frac{1}{2} | H' | \frac{1}{2}, 0 \rangle &= t/\sqrt{2} , \\ \langle 0, \frac{1}{2} | H' | \frac{1}{2}, 0 \rangle &= \frac{1}{2}t . \end{aligned} \quad (4.12)$$

All other matrix elements are either zero or can be deduced from these three by symmetry. Using the matrix elements, we can calculate the first few moments of the energy band for a hole propagating in both the R and AF configurations. The sum of the weighted number of paths are listed in Table II and are seen to be considerably smaller than those for the one-band Hubbard model. Again, the lowest few moments are dominated by the diagrams with no closed loops, and approximate Green's functions for them can be obtained by renormalizing t in (2.26) by $\sqrt{3}/2$ and $1/\sqrt{2}$

TABLE II. Weighted number of paths with (A_i^J) and without (A_i) intra-atomic exchange.

Configuration	A_i^J	A_i	A_i^J	A_i
	R	R	AF	AF
$l=2$	$4\frac{1}{2}$	6	3	6
$l=4$	$42\frac{3}{8}$	72	$17\frac{1}{4}$	66

for the R and AF configurations, respectively. Clearly, there will also be tails extending out to the full bandwidth $\pm zt$ in this case as previously, and the remarks in Sec. IV A regarding t^2/U terms will qualitatively continue to apply. The net result is that the bulk of the band is narrowed considerably more than in the one-band Hubbard model, the total narrowing being of order 50% in the AF configuration and 35% in the R configuration, for the two-band model considered here.

The results for the bandwidth obtained here are similar to what one obtains using the model of De Gennes,¹⁸ in which an extra conduction electron moves in a conduction band interacting via intra-atomic exchange with a set of localized spins when quantum-mechanical effects²¹ are properly treated. De Gennes treated the localized spins classically, and this leads to the result that the conduction electron cannot hop (except for zero-point fluctuations) in the AF arrangement. Our results would eventually go over to those of De Gennes if there were a large number of electrons per atom. In NiO there are only two electrons in the e_g bands and, therefore, the maximum effect of intra-atomic exchange is the narrowing calculated here. In the language of small polaron mobility calculations,²² this means that the hopping frequency W_0 of a hole is reduced by at most a factor of 2. Heikes²³ and Appel²² have given a classical treatment of this quantity, and Appel has estimated that W_0 will be reduced by a factor of 10 at room temperature in NiO. It is clear from the above result that there are important quantum-mechanical corrections to W_0 . The picture of a "spin polaron" suggested by De Gennes and discussed further by Austin and Mott³ only holds when the spin cloud extends over many atomic distances, since a hole cannot be localized on one or two sites by any spin configuration. The spin polaron is therefore unlikely to ever be a "small polaron."

V. COMPARISON WITH EXPERIMENT

In this paper the character of the spectral function or energy band for the creation of a single hole has been investigated for the half-filled Hubbard model in the atomic limit. The composite picture of the band shape which we obtain is that the bandwidth is narrowed by 20–25%, but that there are tails extending down to the full width of the free band $\pm zt$. Judging from the moments, the approximate Green's function obtained by summing all walks which contain no closed loops gives a good representation of the bulk of the band. The validity of keeping only these walks in calculating the mobility of a small number of carriers is more difficult to judge, especially in view of the cancella-

tion between different walks in evaluating the Kubo formula. One can calculate a few of the lower-order graphs and examine the corrections to the mobility. We find that they are small for the AF configuration, but non-negligible for the R configuration. This result is similar to the analysis of the band shapes in Sec. II. It is interesting that the values of the mobilities obtained are close to those seen experimentally in materials such as NiO. Several authors^{2,3} have argued that the low observed mobilities imply small polaron formation in these materials. While in our model calculations we have ignored all ionic effects, and, therefore, all possible polaron effects, we feel that the low values we obtain for the mobility indicate that one may have to reexamine the arguments in favor of small polarons.

Another interesting comparison with experiment is with the dioxide and sesquioxide series with electronic configurations d^1 , d^2 , d^3 , respectively.¹ The behavior of these materials is discussed by McWhan and Remeika.²⁴ As one moves across the series, there is clearly a transition from paramagnetic bandlike behavior (VO_2 and Ti_2O_3) to antiferromagnetic insulating behavior (MnO_2 and Cr_2O_3). In the sesquioxides the Mott transition occurs in V_2O_3 .²⁵ In the dioxide series the corresponding member CrO_2 is a metallic ferromagnet.¹ It is likely that the basic band to localized transition occurring with increasing number of d electrons may be aided by the narrowing effect on the bands due to increasing intraatomic exchange energies as we go across the series. From this point of view the metallic ferromagnetic behavior of CrO_2 appears less anomalous. In these oxide series we expect that $zt \sim U$. Under such circumstances, if we try to stabilize the ferromagnetic state in an insulator, we will lose all band narrowing. This makes it likely that any ferromagnetic arrangement is metallic. Empirically it appears that the magnetic instability of the metallic phase at the critical boundary is towards ferromagnetism rather than itinerant antiferromagnetism. This raises the very interesting and open question of why, in the dioxides, we have an intermediate metallic ferromagnetic phase, while in the sesquioxides we have a direct transition from an insulating antiferromagnetic phase to a paramagnetic metallic phase.

Note added in proof. Recently N. Ohata and R. Kubo [J. Phys. Soc. Japan 28, 1402 (1970)] have calculated the high-temperature mobility by calculating the moments of the frequency-dependent conductivity. Their value of the dc conductivity is within a factor of 2 of our result (3.15). Using their technique they also calculated the magnetoresistance and found a large negative magnetoresistance.

ACKNOWLEDGMENTS

The authors would like to acknowledge a number

of useful conversations with P. W. Anderson, E. I. Blount, C. Herring, and D. B. McWhan.

¹D. Adler, in *Solid State Physics*, edited by F. Seitz, D. Turnbull, and H. Ehrenreich (Academic, New York, 1968), Vol. 21, p. 1.

²J. Appel, in Ref. 1, p. 193.

³I. G. Austin and N. F. Mott, *Advan. Phys.* **18**, 41 (1969).

⁴J. Hubbard, *Proc. Roy. Soc. (London)* **A276**, 238 (1963); **A281**, 401 (1964).

⁵A. B. Harris and R. V. Lange, *Phys. Rev.* **157**, 295 (1967).

⁶Y. Nagaoka, *Solid State Commun.* **3**, 409 (1965); *Phys. Rev.* **147**, 392 (1966).

⁷P. W. Anderson, *Phys. Rev.* **115**, 2 (1959).

⁸D. M. Esterling and R. V. Lange, *Rev. Mod. Phys.* **40**, 790 (1968); *Phys. Rev.* **B1**, 2231 (1970).

⁹C. Domb, *Advan. Phys.* **9**, 245 (1960).

¹⁰P. W. Anderson, *Phys. Rev.* **109**, 1492 (1958).

¹¹We are grateful to Dr. P. W. Anderson for drawing our attention to the applicability of this technique to the problem at hand.

¹²E. Lieb and F. Y. Wu, *Phys. Rev. Letters* **20**, 1445 (1968).

¹³J. Linderberg and E. W. Thalstrup, *J. Chem. Phys.* **49**, 710 (1968).

¹⁴I. M. Lifshitz, *Advan. Phys.* **13**, 483 (1969).

¹⁵L. N. Bulaevskii and D. I. Khomskii, *Zh. Eksperim. i Teor. Fiz.* **52**, 1603 (1967) [*Soviet Phys. JETP* **25**, 1067 (1967)]; *Fiz. Tverd. Tela* **9**, 3070 (1967) [*Soviet Phys. Solid State* **9**, 2422 (1968)].

¹⁶R. Kubo, *Can. J. Phys.* **34**, 1274 (1956).

¹⁷M. H. Cohen (unpublished).

¹⁸P. G. De Gennes, *Phys. Rev.* **118**, 141 (1960).

¹⁹We are grateful to C. Herring for first presenting this argument to us.

²⁰See, for example, T. Moriya, in *Theory of Magnetism in Transition Metals*, edited by W. Marshall (Academic, New York, 1967).

²¹P. W. Anderson and H. Hasegawa, *Phys. Rev.* **100**, 675 (1955).

²²J. Appel, *Phys. Rev.* **141**, 506 (1966).

²³R. Heikes, in *Transition Metal Compounds*, edited by E. R. Schatz (Gordon and Breach, New York, 1964).

²⁴D. B. McWhan and J. P. Remeika, *Phys. Rev.* (to be published).

²⁵D. B. McWhan, T. M. Rice, and J. P. Remeika, *Phys. Rev. Letters* **23**, 1384 (1969).

Nonlinear Spin-Wave Theory for the Anisotropic Heisenberg Antiferromagnet

L. Flax

Lewis Research Center, Cleveland, Ohio 44135

and

John C. Raich

Colorado State University, Fort Collins, Colorado 80520

(Received 27 March 1970)

The theory of the anisotropic Heisenberg antiferromagnet is developed in the nonlinear spin-wave approximation. It is shown that the thermodynamic quantities of interest depend on two renormalization parameters. These parameters can be calculated analytically over the entire temperature range of interest. It appears that nonlinear spin-wave theory does not give a good estimate of the transition temperature as the anisotropy increases.

INTRODUCTION

One of the most important methods in studying the thermodynamic behavior of ferromagnetism or antiferromagnetism is by spin-wave theory, first initiated by Bloch.¹ The assumption is that spin-wave excitations do not interact. By the use of a Holstein-Primakoff transformation the spin-wave operators can be cast into the form of boson operators. This description of the system in terms of noninteracting bosons loses its validity as the temperature is increased. The theory suffers from the drawback that its applicability is limited to a narrow range of temperatures.

With the use of a suitable transformation, Dyson²

transformed the Hamiltonian of spin operators into a boson form which consisted of quadratic and quartic operators. The quadratic part yielded the Bloch spin-wave theory, and the nonquadratic part leads the now famous T^4 term in the magnetization. He was therefore able to calculate the effects of spin-wave interaction for the Heisenberg ferromagnet.

Bloch³ extended the regions of applicability of the spin-wave theory by truncating Dyson's Hamiltonian and finding solutions at higher temperatures.

Liu⁴ extended the Bloch theory to a Heisenberg antiferromagnet. Using Green's-function formalism, the model was studied at high temperatures for spin-wave interactions. It was shown that the